Highlights

1. Plant waxes of the drought-tolerant conifer *Juniperus monosperma* were studied
2. Temperature (T) and precipitation (P) were manipulated for mature trees
3. Higher T resulted in greater *n*-alkane concentrations, but not for other waxes
4. Decreased P did not affect plant wax concentrations
5. Average chain length (ACL) was not affected by T or P

Plant wax and carbon isotope response to heat and drought in the conifer *Juniperus monosperma*

Aaron F. Diefendorf [a*], Christopher P. Bickford [b], Kristen M. Schlanser [a], Erika J. Freimuth [a], Jeffrey S. Hannon [a], Charlotte Grossiord [c,d], and Nate G. McDowell [d,e]

[a] *Department of Geology, University of Cincinnati, Cincinnati, OH, 45221 USA*

[b] *Department of Biology, Kenyon College, Gambier, OH, 43022*

[c] *Plant Ecology Research Laboratory, School of Architecture, Civil and Environmental Engineering, EPFL, Lausanne, Switzerland*

[d] *Functional Plant Ecology, Community Ecology Unit, Swiss Federal Institute for Forest, Snow and Landscape Research (WSL), Lausanne, Switzerland*

[d] *Atmospheric Sciences and Global Change Division, Pacific Northwest National Lab, PO Box 999, Richland, WA, 99352*

[e] *School of Biological Sciences, Washington State University, PO Box 644236, Pullman, WA 99164-4236*

[*]Corresponding Author. Tel. : +1-513-556-3787.

E-mail address: aaron.diefendorf@uc.edu (A.F. Diefendorf).

Keywords: plant biomarker; gymnosperm; leaf wax; compound-specific isotope analysis

Abstract

Plant waxes, including *n*-alkanes, are commonly used for a wide range of paleo applications. Several common traits of *n*-alkanes that are used as paleo proxies include chain length distribution and average chain length (ACL), as well as plant wax carbon and hydrogen isotopic compositions. The effect of climate on plant wax traits has been the subject of many studies, but a common challenge with modern calibrations is disentangling species (genetic), temperature, and precipitation from one another. Here, we explore the effect of temperature and drought, independently and combined, on plant wax composition of the species *Juniper monosperma* in a large ecosystem-scale field manipulation experiment. We find that *n*-alkane concentrations significantly increase with temperature, but other parameters (including ACL) are not affected. These results support physiological studies that identify *n*-alkanes as an important barrier to water loss within the plant cuticle. Combined with prior studies, it appears that changes in ACL within sediments are likely controlled by changes in species composition rather than directly by changes in climate. We find little variation in the carbon isotopic composition ($\delta^{13}C$) of *n*-alkanes across the treatments whereas bulk leaf $\delta^{13}C$ values are higher in the heat and drought treatment. Because leaf $\delta^{13}C$ values represent a weighted C assimilation signal, these values reflect differences in leaf gas exchange among treatments, whereas the *n*-alkanes are synthesized when water availability is higher and differences among treatments are not significant enough to influence their values. These results have important implications for using *n*-alkane traits, including ACL and $\delta^{13}C$ values, for paleoenvironmental reconstructions.

1. Introduction

Plant waxes contain a mix of aliphatic long-chain *n*-alkyl compounds including *n*-alkanes, *n*-alkanols, and *n*-alkanoic acids (Eglinton et al., 1962; Eglinton and Hamilton, 1963, 1967; Kunst and Samuels, 2003; Jetter et al., 2006). *n*-Alkanes, a common constituent of plant wax, is the focus of most studies as they are well preserved in the geologic record, are useful for paleoclimate applications, and are relatively easy to analyze (Castañeda and Schouten, 2011; Freeman and Pancost, 2014; Diefendorf and Freimuth, 2017; Berke, 2018). Typically, terrestrial plant-derived *n*-alkanes have chain lengths that range from *n*-C_{25} to *n*-C_{35} with a strong odd over even preference. The most abundant chain lengths depend strongly on plant growth form, major taxonomic group, and species (e.g., Diefendorf and Freimuth, 2017). The function of plant wax is primarily to limit plant water loss through the cuticle, but it also has important functions in limiting UV exposure and for pathogen defense (Riederer and Schneider, 1990; Riederer and Markstadter, 1996; Jetter et al., 2000; Riederer and Schreiber, 2001; Muller and Riederer, 2005; Koch and Ensikat, 2008; Jetter and Riederer, 2016; Schuster et al., 2016; Zeisler-Diehl et al., 2018). In desert plants, waxes limit water loss by forming a highly ordered wax barrier in concert with triterpenoids to limit water loss, even for high ambient temperatures (Jetter and Riederer, 2016; Schuster et al., 2016). Because plant waxes are involved in limiting water loss, studies have postulated that climate will influence the chemical composition of plant waxes, especially the amount and chain length of *n*-alkyl compounds, as these modify cuticle function and therefore can be used for paleo applications (e.g., Riederer and Schneider, 1990; Koch and Ensikat, 2008; Bush and McInerney, 2013; Hoffmann et al., 2013; Bush and McInerney, 2015; Feakins et al., 2016; Diefendorf and Freimuth, 2017; Andrae et al., 2019).

Studies that have investigated the role of climate on plant wax composition and function have found competing observations. In modern field-based studies of plants and soils, *n*-alkane composition sometimes tracks aridity and/or temperature. In many transect or altitudinal studies, species composition is mixed, unknown, or changes along with climate (e.g., Körner, 2007). For example, in a large study of 158 species along a topical elevation transect, increasing altitude correlated with an increase in *n*-alkane concentration and a decrease in ACL values (Feakins et al., 2016). These studies are informative as they are likely more relevant for paleo applications that focus on sediments that integrate waxes from many species. In a few species-specific studies, climate is shown to influence the *n*-alkane composition. For example, Tipple and Pagani (2013) found a small, but significant increase in the most abundant *n*-alkane chain length with increasing temperature along with a large latitudinal study of *Acer rubra* and *Juniperus virginiana*. In contrast, Andrae et al. (2019) found that the most abundant chain length and overall concentration of *n*-alkanes in *Melaleuca quinquenervia* are similar along continuous climate gradients. Instead, Andrae et al. (2019) observed that isolated populations of the same species were unique, suggesting that species adapt when geographically isolated and this may or may not be associated with climate. Plant waxes also vary through the growing season, suggesting some influence of climate on wax composition (Sachse et al., 2009; Tipple et al., 2013; Freimuth et al., 2017; Suh and Diefendorf, 2018). Combined, *n*-alkane behavior may suggest a species-dependent phenotypic response to climate and could explain why *n*-alkanes respond to temperature in some species, but not in others. A significant challenge with these field-based studies is rigorously evaluating the independent effects of temperature and precipitation, especially when other factors, such as altitude or species, are also varied.

The effects of temperature and precipitation, or drought, on the carbon isotopic composition ($\delta^{13}C$) of bulk leaves ($\delta^{13}C_{leaf}$) is the focus of numerous studies with wide ranging applications for modern and past changes in biology, ecology, and geology (e.g., Tipple and Pagani, 2007; Diefendorf et al., 2010; Kohn, 2010). For plants that utilize the C_3 photosynthetic pathway (e.g., angiosperm trees, many grasses, and conifers), the effects of temperature on $\delta^{13}C_{leaf}$ is challenging to tease apart from other environmental controls, or species turnover, that covary with temperature, especially in studies that utilize altitudinal gradients (Körner, 2007). The effects of precipitation on $\delta^{13}C_{leaf}$ highlight that increasing precipitation causes a nonlinear increase in carbon isotope fractionation during photosynthesis, and thus a lowering of $\delta^{13}C_{leaf}$ values (e.g., Diefendorf et al., 2010; Kohn, 2010). Variations in $\delta^{13}C_{leaf}$ values are of particular interest for geologic studies because they are useful for constraining past changes in climate, vegetation, and the carbon cycle (Freeman and Pancost, 2014; Diefendorf and Freimuth, 2017; Schlanser et al., 2020a). However, unaltered leaf material is rarely preserved in both recent and geologic age sediments. Materials related to the leaf are often analyzed instead, such as leaf macrofossils, cuticles, or plant-derived biomarkers, including long-chain *n*-alkanes. The $\delta^{13}C$ values of *n*-alkanes are related to $\delta^{13}C_{leaf}$ values because both materials are synthesized primarily from C fixed during photosynthesis (Hayes, 2001; Chikaraishi et al., 2004; Diefendorf et al., 2011; 2015b). To relate the $\delta^{13}C$ values of these two materials, especially for geologic applications, the carbon isotope fractionation between leaf and *n*-alkane is often measured in modern studies and applied in geologic studies using epsilon notation, where:

$$\varepsilon^{13}C_{n\text{-alkane}} = \left(\frac{\delta^{13}C_{n\text{-alkane}} + 1}{\delta^{13}C_{leaf} + 1} - 1\right) \qquad \text{Eq. 1}$$

This is not a true reactant/product relationship as the route from photosynthetic C in glucose to leaf or *n*-alkane is complicated by many biosynthetic pathways and their unique isotope effects

(Deines, 1980). In modern C_3 trees, $\delta^{13}C_{n\text{-alkane}}$ values vary by chain length and are also controlled by species, growth form, photosynthetic pathway, and possibly climate, or at least factors that covary with climate (Diefendorf and Freimuth, 2017). Within a species, *n*-alkane $\delta^{13}C$ values generally track $\delta^{13}C_{leaf}$. However, this relationship is not perfect. *n*-Alkanes are synthesized early in the growing season, or when water is available (Sachse et al., 2009; Tipple et al., 2013; Freimuth et al., 2017; Suh and Diefendorf, 2018). This contrasts with $\delta^{13}C_{leaf}$, which is weighted by C assimilation (e.g., Ehleringer et al., 1992; Seibt et al., 2008). Few studies have investigated the role of climate on *n*-alkane $\delta^{13}C$ values or $\varepsilon^{13}C_{n\text{-alkane}}$, especially where climate and/or species are controlled for (Pedentchouk et al., 2008; Wu et al., 2017). This is critical for geologic studies as the controls on and variability in $\varepsilon^{13}C_{n\text{-alkane}}$ need to be constrained for utilizing *n*-alkane $\delta^{13}C$ values as recorders of plant carbon isotope fractionation during photosynthesis.

To explore the effects of temperature and drought on plant biomarkers from a single species independent of spatial variability, we use an ecosystem-scale manipulation experiment in a piñon-juniper woodland in northern New Mexico (Adams et al., 2015; Garcia-Forner et al., 2016; Grossiord et al., 2017a; 2017b; 2017c; McBranch et al., 2018; McDowell et al., 2019). Native mature *Juniperus monosperma*, a genera of conifers that make substantial concentrations of *n*-alkanes (Diefendorf et al., 2015b), were subjected to increased temperature (+4.8 ºC) and/or drought (~45% precipitation reduction) for four years. We evaluated these climate effects on plant wax concentration and chain lengths for *n*-alkanes, *n*-alkanols, and *n*-alkanoic acids. We also analyzed these climate effects on $\delta^{13}C_{leaf}$ and *n*-alkane $\delta^{13}C$ values. We also imaged the needle surfaces to explore any morphological changes among the treatments using a scanning electron microscope (SEM). This approach provides a way to determine if the short-term (years)

changes in temperature and drought influence plant wax composition, and $\delta^{13}C$ values, and avoids the influence of genetic changes (e.g., Tipple and Pagani, 2013; Andrae et al., 2019) within a species along climatic gradients.

2. Materials and methods

2.1. Location, growth treatment, and sample preparation

Samples were collected from *Juniperus monosperma* (Engelm.) Sarg. (juniper) growing at the Los Alamos Survival–Mortality (SUMO) field study located in Los Alamos County, New Mexico (35.49º N, 106.18º W, 2175 m a.s.l.). At this site, the woodland is dominated by piñon pine (*Pinus edulis*) and juniper. Additional minor species include grasses, cacti, the shrubby Gambel oak (*Quercus gambelii*), and ponderosa pine (*Pinus ponderosa*). The soils at this site are derived from volcanic tuffs forming Hackroy clay loam soils that are 40 to 80 cm thick (http://websoilsurvey.nrcs.usda.gov). The mean annual temperature (MAT) is 9.2 ºC (years 1987 to 2011) and the mean annual precipitation is 415 mm (years 1987 to 2012). Due to the North American Monsoon, half of this precipitation falls during thunderstorms from July through September (climate data from http://environweb.lanl.gov/weathermachine). Additional information about the site, plant physiology, and experimental design is reported elsewhere (Adams et al., 2015; Garcia-Forner et al., 2016; Grossiord et al., 2017a; 2017b; 2017c; McBranch et al., 2018; McDowell et al., 2019).

At this site, trees were selected for a manipulative study using open-top chambers and a rain shelter to examine the effects of drought and heat on *P. edulis* and *J. monosperma*. For leaf wax analysis, we selected only *J. monosperma* as the *P. edulis* has very low *n*-alkane

156 concentrations (Diefendorf et al., 2015b). Selected *J. monosperma* trees were between 1.5 and
157 4.5 m tall and the mean tree age was 79 ± 7 years. In this study, a minimum of six tree replicates
158 were assigned to each of the five treatments: (1) ambient control with trees growing in the open
159 (no manipulation; 'ambient control'), (2) chambers with no manipulation, to test for ambient
160 chamber effects ('chamber control'), (3) chambers with heat applied ('heat'), (3) trees growing
161 in the open, but under a rain shelter to simulate drought conditions ('drought'), and (5) chambers
162 with heat and where trees are located under a rain shelter to simulate drought ('heat+drought').
163 Manipulations started in June 2012 and continued for five years.

164 Chambers were open at the top and ranged in footprint area from 6 to 20 m^2. Each
165 chamber contained up to five trees located at a minimum distance of 1.5 m from the chamber
166 wall. Examples of these chambers are shown in Grossiord et al. (2017a). Climate conditions
167 including temperature and relative humidity were continuously monitored for ambient conditions
168 and inside the chambers. Plant leaf gas exchange, vapor pressure deficit, soil water
169 characteristics, along with many other plant, environmental, and edaphic variables were also
170 measured (Adams et al., 2015; Garcia-Forner et al., 2016; Grossiord et al., 2017a; 2017b).
171 Chamber air temperatures were controlled with industrial-scale heat ventilation and air
172 conditioning systems (HVAC). Chamber temperatures were maintained at ambient for the
173 chamber control and at 4.8 ºC above ambient for the heat and heat+drought treatments.

174 Trees in the drought manipulations, located in the open or in chambers, were situated
175 under a precipitation exclusion structure that consisted of clear polymer troughs that reduced
176 precipitation by covering 45% of the overhead surface area. Troughs extended a minimum of 10
177 m outward from the trees. This distance is two times the height of the tallest tree in the drought
178 treatment to ensure that the majority of tree roots were contained within the drought

manipulation zone (Grossiord et al., 2017a). Temperature and precipitation manipulation amounts were selected to match projected values from climate change models for the year 2100 using a business-as-usual scenario (Pachauri et al., 2014).

The effects of heating and drought on *J. monosperma*, along with other species at this site, were summarized extensively elsewhere (Adams et al., 2015; Garcia-Forner et al., 2016; Grossiord et al., 2017a; 2017b; 2017c; McBranch et al., 2018; McDowell et al., 2019). In brief, under a five-year reduction in precipitation and increased heat, the plants experienced severe conditions associated with increased temperature and vapor pressure deficits altering carbon and water metabolism (Adams et al., 2015; 2017). Despite this, carbon starvation and hydraulic failure was minor and no trees in the experiment died. This was primarily attributed to the increased uptake of groundwater (McDowell et al., 2019).

For this study, branch samples (~15 cm long) were collected from the distal foliar clump on the south-facing side of the trees at chest height in July and August of 2016 (Year 4 of the study). This sampling strategy is informed from needle emergence studies at this site (Adams et al., 2015). The total number of individuals varied by treatment from 4 to 8 (Table 1). Branch samples (~10 g) were frozen, subsequently dried at 40 to 45 ºC and stored in paper bags. Needles were subsampled (~1 g) from branches and powdered with a ball mill. Replicate sampling was completed on most samples by additional subsampling of needles from the branch samples. Powdered samples were split for $\delta^{13}C_{leaf}$ analysis and leaf wax extraction. Additional samples were collected from the dried branch samples for SEM imagining.

2.2. Extraction and fractionation

Powdered leaves were extracted using an accelerated solvent extractor (Dionex ASE 350) with 2:1 (v/v) DCM/MeOH. For a subset of samples, 5 µg of 5α-androstane was added as a recovery standard. Samples were then evaporated with N_2. The total lipid extract (TLE) was base saponified with 2.5 mL 0.5 N KOH in 3:1 (v/v) MeOH/water for 2 h at 75 °C. After cooling, 2 mL of NaCl in water (5%, w/w) was added and then the solution was acidified with 6 N HCl to a pH of 1. The acidic solution was extracted with hexanes/DCM (4:1, v/v), neutralized with $NaHCO_3/H_2O$ (5%, w/w), and dried with Na_2SO_4. The saponified lipid extract was subsequently separated into four polarity fractions (Sessions, 2006; Diefendorf et al., 2015b) with 0.5 g of aminopropyl-bonded silica gel. Hydrocarbons were eluted with 4 mL of hexanes, ketones eluted with 8 mL of hexanes/DCM (6:1, v/v), alcohols eluted with 8 mL of DCM/acetone (9:1, v/v), and acids eluted with 8 mL of DCM/formic acid (49:1, v/v). The hydrocarbon fraction was further purified with 1 g of Al_2O_3 and eluted with 4 mL of 9:1 hexanes/DCM (v/v).

2.3. Lipid assignment and quantification

Lipids were identified and quantified on an Agilent 7890A gas chromatograph (GC) interfaced to an Agilent 5975C quadrupole mass selective detector (MSD) and flame ionization detector (FID). Compounds were separated on a fused silica capillary column (Agilent J&W DB-5ms; 30 m length, 0.25 mm i.d., 0.25 µm film thickness) with a guard column (Restek Rxi, 5 m, 0.32 mm). Column effluent was split (1:1) between the FID and MSD with a 2-way splitter with He makeup to keep the pressure constant. For hydrocarbons, the oven program was as follows: 60 °C for 1 min, followed by a ramp (6 °C min^{-1}) to 320 ºC and held for 15 minutes. For ketone, alcohol, and acid fractionations, the oven program was as follows: 60 °C for 1 min, followed by a ramp (20 °C min^{-1}) to 130 °C, then a ramp (4 °C) to 320 °C and held for 10 min. Compounds

were identified with authentic standards, library databases (NIST 2008 and Wiley 2009), spectral interpretation, and by retention time.

For quantification by FID, the hydrocarbon fraction was dissolved quantitatively in hexanes spiked with 25 μg mL^{-1} 1-1'-binapthyl as the internal standard. Aliquots of the ketone, alcohol, and acid fractions were dissolved in pyridine spiked with 25 μg mL^{-1} of 2-dodecanol as the internal standard. Samples were derivatized with *N*,*O*-bis(trimethylsilyl)trifluoroacetamide (BSTFA; Sigma Aldrich) at 70 ºC for 15 min. Compound peak areas were normalized to the response of the internal standard and converted to mass with external standard response curves. External standards for the hydrocarbons were a mix of *n*-alkanes from C_7 to C_{40} (Sigma Aldrich). External standards for the alcohol and acid fractions were a mix of *n*-alkanols (C_{16}, C_{18}, C_{22}, C_{26}, C_{28}) and *n*-alkanoic acids (C_{10}, C_{14}, C_{16}, C_{18}, C_{24}, C_{26}, C_{28}, C_{30}), respectively.

For the *n*-alkanes, precision and accuracy were determined on an in-house *n*-alkane standard (C_{29} and C_{31}) prepared from oak leaves (Oak-1a) which had a weighted mean precision of 4.4 μg mL^{-1} (1σ; 3.4% relative standard deviation, RSD) and an accuracy of –2.3 μg mL^{-1} (–1.8% relative error, RE). For the *n*-alkanols, the weighted (n = 7) mean precision was 2.7 μg mL^{-1} (1σ, 5.3% RSD) and a mean accuracy of –0.3 μg mL^{-1} (–0.5% RE). For the *n*-alkanoic acids, the weighted (n = 7) mean precision was 4.1 μg mL^{-1} (1σ, 8.2% RSD) and a mean accuracy of 0.5 μg mL^{-1} (0.9% RE). Recovery of 5α-androstane was on average 90% (1σ = 5.6% RSD, n = 13). Compound concentrations were normalized to the dry leaf mass (μg g^{-1}).

To compare *n*-alkane chain lengths, we calculated the average chain length (ACL) metric:

$$\mathrm{ACL}_{m-n} = \sum_{i=m}^{n} \frac{i[C_i]}{[C_i]} \qquad \text{Eq. 2}$$

where *m* and *n* represent the shortest and longest chain length, respectively, *i* represents the number of carbon atoms for each homologue, and *C* is the concentration of the *i n*-alkane. Here we use odd *n*-alkane chain lengths from C_{25} and C_{37}. To characterize differences in odd relative to even chain lengths, we calculated the carbon preference index (CPI) using a modified version of Marzi et al. (1993):

$$\text{CPI} = \frac{\left(\sum_{odd} C_{25-35}\right) + \left(\sum_{odd} C_{27-37}\right)}{2 \text{ x } \left(\sum_{even} C_{26-36}\right)} \qquad \text{Eq. 3}$$

where larger CPI values indicate a greater preference for odd chain lengths.

2.4. Carbon isotope analysis

Compound-specific carbon isotope analyses of the *n*-alkanes was determined by GC-combustion (C)-isotope ratio mass spectrometry (IRMS) at the University of Cincinnati. GC-C-IRMS was performed with a Thermo Trace GC Ultra coupled to an Isolink combustion reactor (Ni, Cu, and Pt wires) and Thermo Electron Delta V Advantage IRMS. Isotopic abundances were determined by normalization with Mix A6 (Arndt Schimmelmann, Indiana University) following Coplen et al. (2006). Carbon isotope accuracy across all standard and sample runs was monitored with co-injected *n*-C_{41} alkane with a precision and accuracy of 0.36‰ (1σ; n = 92) and –0.20‰ (n = 92), respectively. Additionally, an in-house *n*-alkane standard (C_{29}, C_{31}) prepared from oak leaves (Oak-1a) was analyzed with a precision and accuracy of 0.24‰ (1σ; n = 24) and 0.04‰ (n = 24), respectively.

The $\delta^{13}C$ of powdered leaves ($\delta^{13}C_{leaf}$) and their weight percent total organic carbon (wt. % TOC) were determined via continuous flow (He; 120 mL min^{-1}) on a Costech elemental analyzer (EA) interfaced with a Thermo Electron Delta V Advantage isotope ratio mass

spectrometer (IRMS) with a Conflo IV. $\delta^{13}C$ values were corrected for sample size dependency and then normalized to the VPDB scale using a calibration with in-house standards (from –38.26‰ to –11.35‰) following Coplen et al. (2006). Error was determined by analyzing two additional independent standards with a mean weighted precision of 0.03‰ (n = 12; 1σ) and accuracy of –0.05‰ (n = 12).

Fractionation that occurs during *n*-alkane biosynthesis was calculated relative to $\delta^{13}C_{leaf}$, using Eq. 1, for *n*-C_{33} and *n*-C_{35} alkanes, the most abundant *n*-alkanes in this species.

2.5. Analysis and statistics

All individual sample replicates were averaged prior to data analysis and number of replicates per individual are listed in Supplementary Table S1 by analysis type. For statistical analyses, we compared the treatments to their respective control groups. The drought treatment was compared to the ambient control group and the heat and heat+drought treatments were compared to the chamber control group. All analyses in this study were performed using JMP Pro 15.0 (SAS, Cary, USA). Unless otherwise noted, two-tailed t-tests were performed using unequal variances.

2.6. SEM analysis of needle surfaces

Ten samples were selected for SEM analysis with duplicates for each treatment type to determine if there were any needle surface morphological differences among the treatments. From each sample, two needles representing older and younger growth were carefully separated from the distal foliar clump using solvent rinsed forceps. Individual needles were mounted on aluminum stubs with carbon tape and sputter-coated with Au-Pd alloy. Samples were then

imaged using a SCIOS Dual-Beam Scanning Electron Microscope at 5.00 kV. For each sample, the abaxial side of the needles was imaged at 800x and 1.5kx. The adaxial side of the needles was imaged at 65x and 1.2kx. For consistency, all SEM images were taken from the same region of each needle. Some additional images of leaf wax were taken at higher magnification (5kx).

3. Results and Discussion

3.1. Effect of heat and drought on leaf waxes

J. monosperma produces *n*-alkan-1-ols with chain lengths ranging from *n*-C_{20} to *n*-C_{32} with the most abundant chain lengths at *n*-C_{22} and *n*-C_{28} (Fig. 1; Supplementary Table S1). *n*-Alkanol concentrations were similar among treatments (t-test) with an average of 106 µg g^{-1}. These concentrations are very similar to other Cupressoideae (Diefendorf et al., 2015b). The mid-positional alkanol *n*-Octacosan-10-ol was the most abundant plant wax alcohol with concentrations averaging 1653 µg g^{-1} and was similar among treatments (t-test). *n*-Octacosan-10-ol is commonly found in conifers and is known to form plant wax tubules on the surface of the cuticle (Jetter and Riederer, 1994; Koch and Ensikat, 2008). The concentrations in this species are >10 times higher than those observed in other conifers making this species wax composition unique (Diefendorf et al., 2015b).

For the *n*-alkanoic acids, chain lengths ranged from *n*-C_{10} (the lowest chain length quantified) to *n*-C_{30} with total concentrations averaging 95 µg g^{-1} (Fig. 1; Table 1 and Supplementary Table S1). Total concentrations were not significantly different between the treatments (t-test). The most abundant chain lengths were *n*-C_{14}, *n*-C_{16}, *n*-C_{22}, and *n*-C_{24}, and these chain lengths were not significantly different among treatments. The chain-length

315 distributions are similar to other conifers; however, concentrations were ~3 times higher than
316 other Cupressoideae (Diefendorf et al., 2015b).

317 For the *n*-alkanes, *J. monosperma* produces chain lengths ranging from *n*-C_{25} to *n*-C_{37},
318 with a strong odd over even preference, but with concentrations far higher for *n*-C_{33} and *n*-C_{35}
319 (Fig. 2; Table 1 and Supplementary Table S1). These chain lengths are longer than most plants
320 but are similar to other species in Cupressoideae and Callitroideae (Diefendorf et al., 2015b).
321 Concentrations of total *n*-alkanes are similar between the control and drought experiments (t-
322 test). However, total *n*-alkane concentrations are ~70% higher for the heat (1458 μg g^{-1}; t-test, p
323 = 0.003) and the heat+drought (1441 μg g^{-1}; t-test, p = 0.007) experiments compared to their
324 control group (853 μg g^{-1}). The concentrations of these *n*-alkanes are far higher than other
325 conifer species, with the exception of the *Widdringtonia schwarzii*, another drought-tolerant
326 conifer (Diefendorf et al., 2015b).

327 ACL values were similar among the treatments with an average value of 33.4 ± 0.1 (n =
328 30; Fig. 2; Table 1 and Supplementary Table S1). There were no differences between the
329 treatments and their control groups (t-test). Overall, these ACL values are similar to other
330 Cupressoideae, which along with the Callitroideae, are much higher than those in other conifer
331 groups and taxa. The high ACL values in these two groups are thought to be inherited from a
332 common ancestor and would be consistent with ACL values not having any strong functional or
333 adaptive significance (Diefendorf et al., 2015b; Andrae et al., 2019).

334 Overall, the mean CPI is 10.3 (Fig. 2; Table 1 and Supplementary Table S1) which is
335 lower than other Cupressoideae, but similar to or higher than other conifer groups (Diefendorf et
336 al., 2015b). CPI is slightly lower for the drought (mean = 10.0; t-test $p < 0.021$) and the
337 heat+drought (mean = 9.3; t-test $p < 0.0001$) treatments compared to their respective control

groups (means of 10.6 and 11.1, respectively). This difference in CPI is small compared to the variation observed in other conifer taxa and therefore is not useful in geologic applications.

As noted previously, several studies have found ACL relationships with climate, although not always the same relationship, when species are controlled for (Hoffmann et al., 2013; Tipple and Pagani, 2013; Andrae et al., 2019). We may not observe any changes in ACL with temperature or drought because these species are already drought-tolerant and this high ACL reflects an adaptive maximum or possibly because the changes in temperature (4.8 ºC) were not large enough or not for a long enough period of time. However, it is more likely that, at least for this species, ACL is tightly controlled by genetics, possibly because higher ACL values are not feasible to synthesize (>*n*-C_{37} alkanes are rarely reported in the literature; e.g., Diefendorf et al., 2015b) or longer *n*-alkanes and higher ACL values do not result in greater plant fitness.

Overall, the main difference in wax chemistry among the treatments is the increased *n*-alkane concentrations in the heat and heat+drought experiments, but not in the drought experiments. This suggests that increased temperature alone results in increased *n*-alkane concentrations. Increased *n*-alkane concentrations are usually associated with changes in precipitation, elevation, aridity, and not temperature alone (e.g., Hoffmann et al., 2013; Bush and McInerney, 2015; Feakins et al., 2016; Andrae et al., 2019). Based on cuticle membrane physiological studies, increased *n*-alkane concentrations cause a decrease in cuticle transpiration by enhancing the resistance of the cuticle to water diffusion (Riederer and Schneider, 1990; Riederer and Schreiber, 2001; Jetter and Riederer, 2016; Schuster et al., 2016; Zeisler-Diehl et al., 2018). This is also supported by observations of g_{min}, the residual leaf cuticular conductance to water vapor when stomata are closed, which are highly temperature sensitive and non-linear

(Cochard, 2019; Duursma et al., 2019). By adding *n*-alkanes, cuticular conductance and thus, g_{min}, can be reduced with heating.

In this study, ACL is maintained between the treatments, despite large increases in total *n*-alkane concentrations with heating, and therefore ACL does not appear to be important for this species to modify cuticle function under higher temperatures. *J. monosperma* is a drought-tolerant species and the reduction in precipitation in this study either was not significant enough to trigger an *n*-alkane response or *n*-alkanes are already at concentrations that are maximized for mitigating water loss under these arid conditions.

3.2. Spatial differences in plant wax morphology

To investigate the role of treatment on the plant wax composition and morphology, we imaged *J. monosperma* needles with SEM to determine if there were any qualitative changes in the spatial patterns of the plant wax morphology (Fig. 3). Directly linking morphology with wax chemistry was outside the scope of this study and instead, we draw from prior studies that have done this in detail (e.g., Gülz, 1994; Jetter and Riederer, 1994; Barthlott et al., 1998; Koch and Ensikat, 2008).

The morphology of *J. monosperma* wax contrasts between the abaxial (facing away from the stem) and adaxial (facing towards the stem) surfaces (Fig. 3). Additionally, any abaxial surfaces covered by needles have a similar morphology to the adaxial surface. The abaxial surface of *J. monosperma* needles are primarily coated with a smooth wax surface with a crust morphology (Fig. 4). Occasionally, small plates, crust granules, and short tubules are present. Based on other studies, the wax chemistry of these surfaces are most consistent with mixtures of *n*-alkyl lipids and other plant compounds, such as terpenoids (Jetter and Riederer, 1994; Barthlott

et al., 1998; Koch and Ensikat, 2008; Schuster et al., 2016; Zeisler-Diehl et al., 2018). Conifers are associated with significant concentrations of terpenoids in their needles (e.g., Diefendorf et al., 2019) and this species also contains significant concentrations of terpenoids, but are not reported here.

The adaxial and covered abaxial surfaces, in contrast, are coated heavily with tubules, some smooth 'amorphous' surfaces, and occasionally crusts (Fig. 4). The presence of tubules coincides with the locations of stomata. In some cases, these tubules thickly cover the stomata guard cells. The chemistry most commonly associated with tubules are mid-positional alcohols (e.g., *n*-nonacosan-10-ol) or diketones (Jetter and Riederer, 1994; Koch and Ensikat, 2008). Given that we did not detect any diketones, we suspect *n*-nonacosan-10-ol as the primary compound forming the tubules. Tubules made of *n*-noncoasn-10-ol are known to create superhydrophobic coatings (Barthlott et al., 2017).

We did not detect any discernible qualitative differences in the surface wax morphology among treatments. The increased *n*-alkane concentrations with heating are therefore likely associated with an increase in *n*-alkanes in the intracuticular wax. If the *n*-alkanes are important for limiting water loss, possibly due to increased vapor pressure deficit (VPD) with increasing heat, then the *n*-alkanes are likely involved in enhancing the transpirational barrier of the cuticle more so than other *n*-alkyl lipids (e.g., Riederer and Schneider, 1990; Jetter et al., 2006; Schuster et al., 2016). The association of the tubules with the stomata, we speculate, provides superhydrophobic surfaces that prevent occlusion of stomatal pores, possibly in a manner that enhances foliar water uptake (Breshears et al., 2008). Tubules, acting as functional microtrichomes, could also provide other adaptations such as modifying boundary layer dynamics above the stomata and enhancing leaf gas exchange (Bickford, 2016).

406

407 *3.3. Effect of heat and drought on leaf wax biosynthetic fractionation*

408 For *J. monosperma*, $\delta^{13}C_{leaf}$ values vary from –26.3 to –23.8‰ (Fig. 5; Table 2 and
409 Supplementary Table S1). The $\delta^{13}C_{leaf}$ values between the drought treatment and ambient control
410 and the heat and chamber control were not different (t-test). However, the heat+drought (–24.6 ±
411 0.5‰, 1σ) and chamber control (–25.4 ± 0.6‰, 1σ) were different (t-test, $p = 0.008$). The $\delta^{13}C$
412 values of the *n*-C_{33} alkanes were similar among all treatments, although the *n*-C_{35} alkanes were
413 marginally higher for the heat (–30.0 ± 0.5‰, 1σ; $p = 0.045$) and heat+drought (–29.9 ± 0.7‰,
414 1σ; $p = 0.078$) treatments compared to the control (–30.9 ± 0.6‰, 1σ).

415 Carbon isotope fractionation is often measured between the $\delta^{13}C$ values of *n*-alkanes and
416 the bulk leaf tissue. This relationship is not a direct reactant-product relationship but is useful for
417 relating plant-derived *n*-alkane $\delta^{13}C$ values back to $\delta^{13}C_{leaf}$ values for paleo applications
418 (Diefendorf and Freimuth, 2017; Schlanser et al., 2020a; 2020b). *J. monosperma* has $\varepsilon^{13}C_{n\text{-C33 alkane}}$
419 values that range from –6.9 to –4.7‰ with a mean value across all treatments of –5.9 (±0.6,
420 1σ). The $\varepsilon^{13}C_{n\text{-C35 alkane}}$ values are slightly higher than $\varepsilon^{13}C_{n\text{-C33 alkane}}$ values (Table 2). The $\varepsilon^{13}C_{n\text{-C33 alkane}}$
421 values are similar among treatments except for the heat+drought treatment (–6.6 ± 0.2σ),
422 which is lower than the control (–5.6 ± 0.6 1σ; $p < 0.007$). Overall, these $\varepsilon^{13}C_{n\text{-C33 alkane}}$ values are
423 much lower (greater fractionation) than other Cupressaceae species located in California under
424 higher precipitation (–3.6 ± 1.1, 1σ, n=19). When the $\delta^{13}C_{leaf}$ values are compared between these
425 two sites, *J. monosperma* values are much higher in New Mexico than California (3.6‰, t-test, p
426 < 0.0001), which is consistent with water availability influencing $\delta^{13}C_{leaf}$ values (e.g., Diefendorf
427 et al., 2010). This is also consistent with Pedentchouk et al. (2008) that observed other drought-
428 tolerant species have consistent $\delta^{13}C_{n\text{-alkane}}$ values. Given that $\varepsilon^{13}C_{n\text{-alkane}}$ values are conservative

among taxa in Cupressaceae (Diefendorf et al., 2015b), it is likely that these much lower $\varepsilon^{13}C_{n\text{-alkane}}$ values for *J. monosperma* might be the result of decoupling between the timing of when *n*-alkanes are synthesized and when bulk leaf tissue is synthesized. *n*-Alkanes are synthesized when water availability is high, such as during the monsoon season or early in the morning, similar to ontogenetic studies that find leaf waxes being made early in the growing season when water is available (Sachse et al., 2009; Tipple et al., 2013; Freimuth et al., 2017; Suh and Diefendorf, 2018). $\delta^{13}C_{leaf}$ values are assimilation weighted, and are also biased to wet periods, but not to the same extent as the *n*-alkanes (e.g., Ehleringer et al., 1992; Seibt et al., 2008). The heat+drought treatment is the only treatment with higher $\delta^{13}C_{leaf}$ values than the control, suggesting some effect of heating and drought, but the $\delta^{13}C_{leaf}$ values are similar across all studies. The much lower $\varepsilon^{13}C_{n\text{-alkane}}$ values in the heat+drought treatment thus reflect the higher $\delta^{13}C_{leaf}$ values, possibly due to a mismatch in the timing of synthesis of *n*-alkanes compared to the bulk leaf tissue. Alternatively, the heat+drought treatment reflects a change in metabolism, possibly due to increased storage of starch with higher $\delta^{13}C$ values (Cernusak et al., 2009).

If the above conjecturing is correct, then this suggests that conifer leaf waxes are synthesized under favorable (wet) conditions, similar to observations in angiosperms (Sachse et al., 2009; Tipple et al., 2013; Freimuth et al., 2017; Suh and Diefendorf, 2018). However, despite the similarities in *n*-alkane $\delta^{13}C$ values across treatments, *n*-alkane concentrations are higher with increased heating (Fig. 5). This indicates that *n*-alkanes in *J. monosperma* are responding to the environment, by increasing concentrations of *n*-alkanes, with increased heating. However, the synthesis of these compounds is occurring when water is available, thus resulting in similar *n*-alkane $\delta^{13}C$ values. This suggests that some *n*-alkane traits (i.e., concentration) respond to temperature, but chain length (ACL) is strongly controlled by genetics (e.g., Diefendorf et al.,

2015b; Andrae et al., 2019). Additionally, $\delta^{13}C$ values of *n*-alkanes and bulk leaf tissue are not recording the same growing season conditions. This mismatch in the timing between *n*-alkane biosynthesis and bulk leaf tissue may be contributing to the large observed variation in $\varepsilon^{13}C_{n\text{-alkane}}$ values (e.g., Diefendorf and Freimuth, 2017). This implies that the $\delta^{13}C$ of *n*-alkanes are recording a specific time of year and this should be incorporated into their interpretations for paleo applications (e.g., Tipple et al., 2013; Freimuth et al., 2017).

3.4. Implications for the paleoenvironmental studies

Despite large changes in temperature and drought, the plant waxes of *J. monosperma* were unaltered with the exception of a large increase in total *n*-alkane concentrations with heating. Other studies have also observed increases in *n*-alkane concentrations with other factors including altitude and canopy height (Feakins et al., 2016; Suh and Diefendorf, 2018). However, total concentrations are unlikely to be useful for paleoenvironmental applications. In studies where species could be controlled, such as analyses of macrofossils or cuticle, the challenge would be controlling for preservation and the loss of compounds. Preservation can be highly variable within and between depositional environments. When comparing *n*-alkane concentrations of taxa between different sites, it would be nearly impossible to remove preservation effects and therefore differences in concentration could not be attributed to heat. Additionally, the further back in time samples are compared, the challenge would be differentiating genetic differences from climate controls (Andrae et al., 2019). Using this approach on closely related taxa would not be possible either given the large differences in *n*-alkane concentrations among closely related species (Diefendorf et al., 2015b).

n-Alkane ACL values are sometimes used as a proxy for temperature (see Freeman and Pancost, 2014). Here, we observed no change in ACL after 4 years of heating. This contrasts with other studies where samples are collected over long sampling gradients or from geographically isolated populations where genetic variation within a species is likely (Hoffmann et al., 2013; Tipple and Pagani, 2013; Feakins et al., 2016; Andrae et al., 2019). Combined, this suggests that ACL should not be used in species-specific studies (e.g., cuticle, macrofossils) as indicators of temperature. For analyses made on sediments or rocks that incorporate waxes from the flora living in the depositional basin, using ACL as a proxy for temperature is not possible. ACL is highly variable among species, sometimes even very closely related species, and therefore any changes in ACL in sediments (spatially or temporally) are most likely caused by changes in species composition (Diefendorf et al., 2015b). Not all changes in the plant community will however translate into an ACL change. For example, teasing apart changes in the relative abundance of conifers and angiosperms on the landscape can be complicated by differences in ACL and the abundance of *n*-alkanes between these plant groups and, despite large changes in the plant community, ACL is maintained (e.g., Schlanser et al., 2020b). Therefore, a lack of change in ACL is not evidence of no change in the plant community. Even if temperature does influence ACL, those changes tend to be small (e.g., Tipple and Pagani, 2013). Therefore, we argue that ACL is not directly sensitive to paleoclimate, but instead is related to changes in species composition. Changes in species composition is controlled by many factors, which include climate, but this relationship between ACL and climate is not direct. Therefore, we contend that when changes in ACL are observed, it can be informative of floral changes over time, or across a landscape, but using ACL as a temperature proxy is fraught with uncertainty.

The Paleocene-Eocene Thermal Maximum (PETM) provides a good example of these challenges. The PETM is associated with a large carbon cycle perturbation around 55.5 Ma and resulted in global warming on the order of 5 to 8 ºC (McInerney and Wing, 2011). Records of the PETM are known from around the world and many of these sites report *n*-alkanes because their isotopes are useful for understanding the carbon cycle perturbation and changes in hydrology. ACL values across the warming at the onset of the PETM are variable with values increasing (Schouten et al., 2007; Smith et al., 2007; Handley et al., 2008; Baczynski et al., 2016) or decreasing (Tipple et al., 2011; Krishnan et al., 2015). For the sites where floral data is available, it is clear that major floral turnover occurred very quickly at the onset of warming (McInerney and Wing, 2011). Therefore, changes in ACL values can be used as an indicator of floral change. Although this is qualitative, it can be helpful when interpreting other changes. For example, if *n*-alkane $\delta^{13}C$ or $\delta^{2}H$ values are changing along with ACL, then the effects of species change on these isotope signals needs to be accounted for, or ruled out, to maximize signal to (biological) noise in the interpretations made (e.g, Schartman et al., 2020).

As mentioned above, *J. monosperma* had much lower $\varepsilon^{13}C_{n\text{-alkane}}$ values than observed in other closely related Cupressaceae taxa (Diefendorf et al., 2015b). Because *n*-alkane $\delta^{13}C$ values are very similar among treatments despite the drought modification and because these values were lower than might be expected based on the arid climate, it is likely that the *n*-alkanes were synthesized under wetter conditions. This possible decoupling between *n*-alkane and bulk leaf tissue synthesis emphasizes that *n*-alkanes are reflecting the wet growing season and bulk leaf $\delta^{13}C$ values are assimilation weighted and are possibly affected by changes in C storage (Cernusak et al., 2009). This difference in timing is important because it might explain why $\varepsilon^{13}C_{n\text{-alkane}}$ values are so highly variable (e.g., Diefendorf and Freimuth, 2017). Additionally, if

519 timing of synthesis or C storage is genetically controlled, it might also explain why in addition to
520 this variability, $\varepsilon^{13}C_{n\text{-alkane}}$ values can have strong taxonomic overprinting, at least in conifers
521 (e.g., Cupressaceae versus Podocarpaceae). If this is the case, then using $\varepsilon^{13}C_{n\text{-alkane}}$ values to
522 correct from *n*-alkane to leaf values may be adding additional uncertainty and suggests that we
523 may need to calibrate *n*-alkane $\delta^{13}C$ values directly to atmospheric $\delta^{13}C$ values to reduce
524 uncertainty for paleoenvironmental applications (Diefendorf et al., 2015a; Schlanser et al.,
525 2020a).
526
527 **4. Conclusions**
528 We investigated the effects of heat and drought on the plant wax compositions of the
529 conifer *J. monosperma* in an ecosystem-scale manipulation experiment. We found that plant wax
530 concentrations are similar among treatments for all *n*-alkyl lipids except for the *n*-alkanes which
531 have much higher concentrations in the heat and heat+drought treatments, but not in the drought
532 treatment. This suggests that heating is responsible for the increase in *n*-alkane production.
533 Given that we observed no qualitative differences in the epicuticular leaf wax morphology, or
534 other *n*-alkyl lipids, *n*-alkanes are being preferentially added to the intracuticular wax to enhance
535 the cuticular transpiration barrier (e.g., Riederer and Schneider, 1990; Jetter et al., 2006; Schuster
536 et al., 2016), possibly in response to high vapor pressure deficit.
537 Despite having higher *n*-alkane concentrations with increased temperatures, *n*-alkane
538 ACL does not vary between treatments and therefore ACL is tightly controlled, at least for this
539 species over four years, and is, therefore, not related to temperature. Other studies have identified
540 unique leaf wax and ACL strategies to climate. Combined, it seems that species have ACL
541 values that are largely set by their genetics and phylogenetic relationships, and over time, small

variations in ACL occur when species are isolated or spread apart over long distances (Tipple and Pagani, 2013; Andrae et al., 2019).

Similar to other species, *n*-alkanes are likely synthesized during the growing season when water availability is higher. In *J. monosperma*, this results in much lower $\varepsilon^{13}C_{n\text{-alkane}}$ values than other taxa in Cupressaceae. Because *n*-alkane $\delta^{13}C$ values are very similar among treatments, the variability observed in the $\varepsilon^{13}C_{n\text{-alkane}}$ values was likely caused by environmental controls on $\delta^{13}C_{leaf}$, and not *n*-alkane $\delta^{13}C$ values. Given that *n*-alkane $\delta^{13}C$ values are usually set early in the growing season, or when water availability is high, the *n*-alkane $\delta^{13}C$ values are biased to those times, whereas leaf $\delta^{13}C$ values are assimilation weighted and therefore do not represent the same time period. This is an important distinction and needs to be taken into account when comparing or interpreting *n*-alkane and leaf $\delta^{13}C$ values as climate recorders.

Acknowledgements

We thank the Editors John Volkman and Julian Sachs, along with Daniel Nelson and an anonymous reviewer, for their helpful comments and suggestions that improved this study. We thank Megan Brennan, Kelly Grogan, Hans Naake, and Anna Schartman for help with sample preparation. We would also like to thank Melodie Fichenscher at the Advanced Material Characterization Center at the University of Cincinnati for microscopy support. This research was partially supported by the US National Science Foundation (EAR-1229114 and EAR-1636546 to A.F.D.). The SUMO experiment was supported by the Department of Energy, Office of Science.

Appendix A. Supplementary material

Supplementary data to this article can be found online at insert DOI link.

Table S1. All sample information including plant wax concentrations and carbon isotope data.

572 **References**

573

574 Adams, H.D., Collins, A.D., Briggs, S.P., Vennetier, M., Dickman, L.T., Sevanto, S.A., Garcia-
575 Forner, N., Powers, H.H., McDowell, N.G., 2015. Experimental drought and heat can
576 delay phenological development and reduce foliar and shoot growth in semiarid trees.
577 Global Change Biology 21, 4210-4220.
578 Adams, H.D., Zeppel, M.J.B., Anderegg, W.R.L., Hartmann, H., Landhäusser, S.M., Tissue,
579 D.T., Huxman, T.E., Hudson, P.J., Franz, T.E., Allen, C.D., Anderegg, L.D.L., Barron-
580 Gafford, G.A., Beerling, D.J., Breshears, D.D., Brodribb, T.J., Bugmann, H., Cobb, R.C.,
581 Collins, A.D., Dickman, L.T., Duan, H., Ewers, B.E., Galiano, L., Galvez, D.A., Garcia-
582 Forner, N., Gaylord, M.L., Germino, M.J., Gessler, A., Hacke, U.G., Hakamada, R.,
583 Hector, A., Jenkins, M.W., Kane, J.M., Kolb, T.E., Law, D.J., Lewis, J.D., Limousin, J.-
584 M., Love, D.M., Macalady, A.K., Martínez-Vilalta, J., Mencuccini, M., Mitchell, P.J.,
585 Muss, J.D., O'Brien, M.J., O'Grady, A.P., Pangle, R.E., Pinkard, E.A., Piper, F.I., Plaut,
586 J.A., Pockman, W.T., Quirk, J., Reinhardt, K., Ripullone, F., Ryan, M.G., Sala, A.,
587 Sevanto, S., Sperry, J.S., Vargas, R., Vennetier, M., Way, D.A., Xu, C., Yepez, E.A.,
588 McDowell, N.G., 2017. A multi-species synthesis of physiological mechanisms in
589 drought-induced tree mortality. Nature Ecology & Evolution 1, 1285-1291.
590 Andrae, J.W., McInerney, F.A., Tibby, J., Henderson, A.C.G., Hall, P.A., Marshall, J.C.,
591 McGregor, G.B., Barr, C., Greenway, M., 2019. Variation in leaf wax *n*-alkane
592 characteristics with climate in the broad-leaved paperbark (*Melaleuca quinquenervia*).
593 Organic Geochemistry 130, 33-42.

Baczynski, A.A., McInerney, F.A., Wing, S.L., Kraus, M.J., Morse, P.E., Bloch, J.I., Chung, A.H., Freeman, K.H., 2016. Distortion of carbon isotope excursion in bulk soil organic matter during the Paleocene-Eocene thermal maximum. Geological Society of America Bulletin.

Barthlott, W., Neinhuis, C., Cutler, D., Ditsch, F., Meusel, I., Theisen, I., Wilhelmi, H., 1998. Classification and terminology of plant epicuticular waxes. Botanical Journal of the Linnean Society 126, 237-260.

Barthlott, W., Mail, M., Bhushan, B., Koch, K., 2017. Plant Surfaces: Structures and Functions for Biomimetic Innovations. Nano-Micro Letters 9, 23.

Berke, M.A., 2018. Reconstructing Terrestrial Paleoenvironments Using Sedimentary Organic Biomarkers. In: Croft, D.A., Su, D.F., Simpson, S.W. (Eds.), Methods in Paleoecology: Reconstructing Cenozoic Terrestrial Environments and Ecological Communities, Springer International Publishing, pp. 121-149.

Bickford, C.P., 2016. Ecophysiology of leaf trichomes. Functional Plant Biology 43, 807-814.

Breshears, D.D., McDowell, N.G., Goddard, K.L., Dayem, K.E., Martens, S.N., Meyer, C.W., Brown, K.M., 2008. Foliar absorption of intercepted rainfall improves woody plant water status most during drought. Ecology 89, 41-47.

Bush, R.T., McInerney, F.A., 2013. Leaf wax *n*-alkane distributions in and across modern plants: Implications for paleoecology and chemotaxonomy. Geochimica et Cosmochimica Acta 117, 161-179.

Bush, R.T., McInerney, F.A., 2015. Influence of temperature and C_4 abundance on *n*-alkane chain length distributions across the central USA. Organic Geochemistry 79, 65-73.

616 Castañeda, I.S., Schouten, S., 2011. A review of molecular organic proxies for examining
617 modern and ancient lacustrine environments. Quaternary Science Reviews 30, 2851-
618 2891.
619 Cernusak, L.A., Tcherkez, G., Keitel, C., Cornwell, W.K., Santiago, L.S., Knohl, A., Barbour,
620 M.M., Williams, D.G., Reich, P.B., Ellsworth, D.S., Dawson, T.E., Griffiths, H.G.,
621 Farquhar, G.D., Wright, I.J., 2009. Why are non-photosynthetic tissues generally ^{13}C
622 enriched compared with leaves in C3 plants? Review and synthesis of current hypotheses.
623 Functional Plant Biology 36, 199-213.
624 Chikaraishi, Y., Naraoka, H., Poulson, S.R., 2004. Carbon and hydrogen isotopic fractionation
625 during lipid biosynthesis in a higher plant (*Cryptomeria japonica*). Phytochemistry 65,
626 323-330.
627 Cochard, H., 2019. A new mechanism for tree mortality due to drought and heatwaves. bioRxiv,
628 531632.
629 Coplen, T.B., Brand, W.A., Gehre, M., Gröning, M., Meijer, H.A.J., Toman, B., Verkouteren,
630 R.M., 2006. New guidelines for $\delta^{13}C$ measurements. Analytical Chemistry 78, 2439-
631 2441.
632 Deines, P., 1980. The isotopic composition of reduced organic carbon. In: Fritz, P., Fontes, J.C.
633 (Eds.), Handbook of Environmental Isotope Geochemistry, Elsevier, pp. 329-406.
634 Diefendorf, A.F., Mueller, K.E., Wing, S.L., Koch, P.L., Freeman, K.H., 2010. Global patterns in
635 leaf ^{13}C discrimination and implications for studies of past and future climate.
636 Proceedings of the National Academy of Sciences 107, 5738-5743.

637 Diefendorf, A.F., Freeman, K.H., Wing, S.L., Graham, H.V., 2011. Production of *n*-alkyl lipids
638 in living plants and implications for the geologic past. Geochimica et Cosmochimica
639 Acta 75, 7472-7485.
640 Diefendorf, A.F., Freeman, K.H., Wing, S.L., Currano, E.D., Mueller, K.E., 2015a. Paleogene
641 plants fractionated carbon isotopes similar to modern plants. Earth and Planetary Science
642 Letters 429, 33-44.
643 Diefendorf, A.F., Leslie, A.B., Wing, S.L., 2015b. Leaf wax composition and carbon isotopes
644 vary among major conifer groups. Geochimica et Cosmochimica Acta 170, 145-156.
645 Diefendorf, A.F., Freimuth, E.J., 2017. Extracting the most from terrestrial plant-derived n-alkyl
646 lipids and their carbon isotopes from the sedimentary record: A review. Organic
647 Geochemistry 103, 1-21.
648 Diefendorf, A.F., Leslie, A.B., Wing, S.L., 2019. A phylogenetic analysis of conifer diterpenoids
649 and their carbon isotopes for chemotaxonomic applications. Organic Geochemistry 127,
650 50-58.
651 Duursma, R.A., Blackman, C.J., Lopéz, R., Martin-StPaul, N.K., Cochard, H., Medlyn, B.E.,
652 2019. On the minimum leaf conductance: its role in models of plant water use, and
653 ecological and environmental controls. New Phytologist 221, 693-705.
654 Eglinton, G., Gonzalez, A.G., Hamilton, R.J., Raphael, R.A., 1962. Hydrocarbon constituents of
655 the wax coatings of plant leaves: A taxonomic survey. Phytochemistry 1, 89-102.
656 Eglinton, G., Hamilton, R.J., 1963. The distribution of *n*-alkanes. In: Swain, T. (Ed.), Chemical
657 Plant Taxonomy, Academic Press, pp. 197-217.
658 Eglinton, G., Hamilton, R.J., 1967. Leaf epicuticular waxes. Science 156, 1322-1335.

659 Ehleringer, J.R., Phillips, S.L., Comstock, J.P., 1992. Seasonal variation in the carbon isotopic
660 composition of desert plants. Functional Ecology 6, 396-404.
661 Feakins, S.J., Peters, T., Wu, M.S., Shenkin, A., Salinas, N., Girardin, C.A.J., Bentley, L.P.,
662 Blonder, B., Enquist, B.J., Martin, R.E., Asner, G.P., Malhi, Y., 2016. Production of leaf
663 wax *n*-alkanes across a tropical forest elevation transect. Organic Geochemistry 100, 89-
664 100.
665 Freeman, K.H., Pancost, R.D., 2014. Biomarkers for terrestrial plants and climate. In: Holland,
666 K.K., Turekian, H.D. (Eds.), Treatise on Geochemistry (Second Edition), Elsevier, pp.
667 395-416.
668 Freimuth, E.J., Diefendorf, A.F., Lowell, T.V., 2017. Hydrogen isotopes of n-alkanes and n-
669 alkanoic acids as tracers of precipitation in a temperate forest and implications for
670 paleorecords. Geochimica et Cosmochimica Acta 206, 166-183.
671 Garcia-Forner, N., Adams, H.D., Sevanto, S., Collins, A.D., Dickman, L.T., Hudson, P.J.,
672 Zeppel, M.J.B., Jenkins, M.W., Powers, H., Martínez-Vilalta, J., McDowell, N.G., 2016.
673 Responses of two semiarid conifer tree species to reduced precipitation and warming
674 reveal new perspectives for stomatal regulation. Plant, Cell & Environment 39, 38-49.
675 Grossiord, C., Sevanto, S., Adams, H.D., Collins, A.D., Dickman, L.T., McBranch, N.,
676 Michaletz, S.T., Stockton, E.A., Vigil, M., McDowell, N.G., 2017a. Precipitation, not air
677 temperature, drives functional responses of trees in semi-arid ecosystems. Journal of
678 Ecology 105, 163-175.
679 Grossiord, C., Sevanto, S., Borrego, I., Chan, A.M., Collins, A.D., Dickman, L.T., Hudson, P.J.,
680 McBranch, N., Michaletz, S.T., Pockman, W.T., Ryan, M., Vilagrosa, A., McDowell,

N.G., 2017b. Tree water dynamics in a drying and warming world. Plant, Cell & Environment 40, 1861-1873.

Grossiord, C., Sevanto, S., Dawson, T.E., Adams, H.D., Collins, A.D., Dickman, L.T., Newman, B.D., Stockton, E.A., McDowell, N.G., 2017c. Warming combined with more extreme precipitation regimes modifies the water sources used by trees. New Phytologist 213, 584-596.

Gülz, P.-G., 1994. Epicuticular Leaf Waxes in the Evolution of the Plant Kingdom. Journal of Plant Physiology 143, 453-464.

Handley, L., Pearson, P.N., McMillan, I.K., Pancost, R.D., 2008. Large terrestrial and marine carbon and hydrogen isotope excursions in a new Paleocene/Eocene boundary section from Tanzania. Earth and Planetary Science Letters 275, 17-25.

Hayes, J.M., 2001. Fractionation of carbon and hydrogen isotopes in biosynthetic processes. Reviews in Mineralogy and Geochemistry 43, 225-277.

Hoffmann, B., Kahmen, A., Cernusak, L.A., Arndt, S.K., Sachse, D., 2013. Abundance and distribution of leaf wax *n*-alkanes in leaves of Acacia and Eucalyptus trees along a strong humidity gradient in northern Australia. Organic Geochemistry 62, 62-67.

Jetter, R., Riederer, M., 1994. Epicuticular crystals of nonacosan-10-ol: In-vitro reconstitution and factors influencing crystal habits. Planta 195, 257-270.

Jetter, R., Schaffer, S., Riederer, M., 2000. Leaf cuticular waxes are arranged in chemically and mechanically distinct layers: evidence from *Prunus laurocerasus L*. Plant Cell and Environment 23, 619-628.

Jetter, R., Kunst, L., Samuels, A.L., 2006. Composition of plant cuticular waxes. In: Rieder, M., Muller, C. (Eds.), Biology of the plant cuticle, Blackwell Publishing, pp. 145-181.

704 Jetter, R., Riederer, M., 2016. Localization of the transpiration barrier in the epi- and
705 intracuticular waxes of eight plant species: Water transport resistances are associated
706 with fatty acyl rather than alicyclic components. Plant Physiology 170, 921-934.
707 Koch, K., Ensikat, H.J., 2008. The hydrophobic coatings of plant surfaces: Epicuticular wax
708 crystals and their morphologies, crystallinity and molecular self-assembly. Micron 39,
709 759-772.
710 Kohn, M.J., 2010. Carbon isotope compositions of terrestrial C_3 plants as indicators of
711 (paleo)ecology and (paleo)climate. Proceedings of the National Academy of Sciences
712 107, 19691-19695.
713 Körner, C., 2007. The use of 'altitude' in ecological research. Trends in Ecology & Evolution 22,
714 569-574.
715 Krishnan, S., Pagani, M., Agnini, C., 2015. Leaf waxes as recorders of paleoclimatic changes
716 during the Paleocene–Eocene Thermal Maximum: Regional expressions from the
717 Belluno Basin. Organic Geochemistry 80, 8-17.
718 Kunst, L., Samuels, A.L., 2003. Biosynthesis and secretion of plant cuticular wax. Progress in
719 Lipid Research 42, 51-80.
720 Marzi, R., Torkelson, B.E., Olson, R.K., 1993. A revised carbon preference index. Organic
721 Geochemistry 20, 1303-1306.
722 McBranch, N.A., Grossiord, C., Adams, H., Borrego, I., Collins, A.D., Dickman, T., Ryan, M.,
723 Sevanto, S., McDowell, N.G., 2018. Lack of acclimation of leaf area:sapwood area ratios
724 in piñon pine and juniper in response to precipitation reduction and warming. Tree
725 Physiology 39, 135-142.

McDowell, N.G., Grossiord, C., Adams, H.D., Pinzón-Navarro, S., Mackay, D.S., Breshears, D.D., Allen, C.D., Borrego, I., Dickman, L.T., Collins, A., Gaylord, M., McBranch, N., Pockman, W.T., Vilagrosa, A., Aukema, B., Goodsman, D., Xu, C., 2019. Mechanisms of a coniferous woodland persistence under drought and heat. Environmental Research Letters 14, 045014.

McInerney, F.A., Wing, S.L., 2011. The Paleocene-Eocene Thermal Maximum: A perturbation of carbon cycle, climate, and biosphere with implications for the future. Annual Review of Earth and Planetary Sciences 39, 489-516.

Muller, C., Riederer, M., 2005. Plant surface properties in chemical ecology. Journal of Chemical Ecology 31, 2621-2651.

Pedentchouk, N., Sumner, W., Tipple, B., Pagani, M., 2008. $\delta^{13}C$ and δD compositions of n-alkanes from modern angiosperms and conifers: An experimental set up in central Washington State, USA. Organic Geochemistry 39, 1066-1071.

Riederer, M., Schneider, G., 1990. The effect of the environment on the permeability and composition of Citrus leaf cuticles. Planta 180, 154-165.

Riederer, M., Markstadter, C., 1996. Cuticular waxes: a critical assessment of current knowledge. In: Kersteins, G. (Ed.), Plant cuticles: an integrated functional approach, BIOS Scientific Publishers, pp. 189-200.

Riederer, M., Schreiber, L., 2001. Protecting against water loss: analysis of the barrier properties of plant cuticles. Journal of Experimental Botany 52, 2023-2032.

Sachse, D., Kahmen, A., Gleixner, G., 2009. Significant seasonal variation in the hydrogen isotopic composition of leaf-wax lipids for two deciduous tree ecosystems (*Fagus sylvativa* and *Acer pseudoplatanus*). Organic Geochemistry 40, 732-742.

749 Schartman, A.K., Diefendorf, A.F., Lowell, T.V., Freimuth, E.J., Stewart, A.K., Landis, J.D.,
750 Bates, B.R., 2020. Stable source of Holocene spring precipitation recorded in leaf wax
751 hydrogen-isotope ratios from two New York lakes. Quaternary Science Reviews 240,
752 106357.
753 Schlanser, K., Diefendorf, A.F., Greenwood, D.R., Mueller, K.E., West, C.K., Lowe, A.J.,
754 Basinger, J.F., Currano, E.D., Flynn, A.G., Fricke, H.C., Geng, J., Meyer, H.W., Peppe,
755 D.J., 2020a. On geologic timescales, plant carbon isotope fractionation responds to
756 precipitation similarly to modern plants and has a small negative correlation with pCO_2.
757 Geochimica et Cosmochimica Acta 270, 264-281.
758 Schlanser, K.M., Diefendorf, A.F., West, C.K., Greenwood, D.R., Basinger, J.F., Meyer, H.W.,
759 Lowe, A.J., Naake, H.H., 2020b. Conifers are a major source of sedimentary leaf wax n-
760 alkanes when dominant in the landscape: Case studies from the Paleogene. Organic
761 Geochemistry 147, 104069.
762 Schouten, S., Woltering, M., Rijpstra, W.I.C., Sluijs, A., Brinkhuis, H., Sinninghe Damste, J.S.,
763 2007. The Paleocene-Eocene carbon isotope excursion in higher plant organic matter:
764 Differential fractionation of angiosperms and conifers in the Arctic. Earth and Planetary
765 Science Letters 258, 581-592.
766 Schuster, A.-C., Burghardt, M., Alfarhan, A., Bueno, A., Hedrich, R., Leide, J., Thomas, J.,
767 Riederer, M., 2016. Effectiveness of cuticular transpiration barriers in a desert plant at
768 controlling water loss at high temperatures. AoB PLANTS 8, plw027-plw027.
769 Seibt, U., Rajabi, A., Griffiths, H., Berry, J., 2008. Carbon isotopes and water use efficiency:
770 sense and sensitivity. Oecologia 155, 441-454.

771 Smith, F.A., Wing, S.L., Freeman, K.H., 2007. Magnitude of the carbon isotope excursion at the
772 Paleocene-Eocene thermal maximum: The role of plant community change. Earth and
773 Planetary Science Letters 262, 50-65.
774 Suh, Y.J., Diefendorf, A.F., 2018. Seasonal and canopy height variation in n-alkanes and their
775 carbon isotopes in a temperate forest. Organic Geochemistry 116, 23-34.
776 Tipple, B.J., Pagani, M., 2007. The early origins of terrestrial C_4 photosynthesis. Annual Review
777 of Earth and Planetary Sciences 35, 435-461.
778 Tipple, B.J., Pagani, M., Krishnan, S., Dirghangi, S.S., Galeotti, S., Agnini, C., Giusberti, L.,
779 Rio, D., 2011. Coupled high-resolution marine and terrestrial records of carbon and
780 hydrologic cycles variations during the Paleocene–Eocene Thermal Maximum (PETM).
781 Earth and Planetary Science Letters 311, 82-92.
782 Tipple, B.J., Berke, M.A., Doman, C.E., Khachaturyan, S., Ehleringer, J.R., 2013. Leaf-wax *n*-
783 alkanes record the plant–water environment at leaf flush. Proceedings of the National
784 Academy of Sciences 110, 2659-2664.
785 Tipple, B.J., Pagani, M., 2013. Environmental control on eastern broadleaf forest species' leaf
786 wax distributions and D/H ratios. Geochimica et Cosmochimica Acta 111, 64-77.
787 Wu, M.S., Feakins, S.J., Martin, R.E., Shenkin, A., Bentley, L.P., Blonder, B., Salinas, N.,
788 Asner, G.P., Malhi, Y., 2017. Altitude effect on leaf wax carbon isotopic composition in
789 humid tropical forests. Geochimica et Cosmochimica Acta 206, 1-17.
790 Zeisler-Diehl, V., Müller, Y., Schreiber, L., 2018. Epicuticular wax on leaf cuticles does not
791 establish the transpiration barrier, which is essentially formed by intracuticular wax.
792 Journal of Plant Physiology 227, 66-74.
793

794

795 **Figures Captions**

796 **Figure 1.** *n*-Alkanol (even chains from C_{20} to C_{32}, *n*-nonacosan-10-ol, and *n*-alkanoic acid (even
797 chains from C_{22} to C_{30}) concentrations ($\mu g\ g^{-1}$) by growth treatment. Samples are represented
798 using box and whisker plots with the median, upper and lower quartiles, and maximum and
799 minimum values indicated. Median values are indicated next to box plots.

800

801 **Figure 2.** *n*-Alkane concentrations (C_{25} to C_{37}; $\mu g\ g^{-1}$), CPI, and ACL values by growth
802 treatment. Samples are represented using box and whisker plots with the median, upper and
803 lower quartiles, and maximum and minimum values indicated. Median values are indicated next
804 to box plots.

805

806 **Figure 3.** SEM images of *J. monosperma* leaves from the ambient control treatment. Image A
807 (J123, 65x) captures multiple needles showing general needle morphology. Image B (J124;
808 350x) captures the exposed adaxial surface when the leaf is separated from the stem thereby
809 revealing the adaxial leaf waxes.

810

811 **Figure 4.** SEM images of *J. monosperma* leaf surface features. Image A (J128; 65x; chamber
812 control) captures wax crusts on the abaxial surface. These crusts may be noticeably apparent due
813 to the drying of the leaves, but capture the thickness of these smooth wax layers. Image B (J117;
814 120x; heat) highlights the difference in leaf wax morphology when a needle is moved (left
815 needle was slid to the left) to expose the normally covered abaxial surfaces. Note the change in
816 morphology of the wax (see E) and the presence of stomata. Image C (J123, 1.2kx; ambient
817 control) provides a view of the smooth wax of the abaxial surfaces see in A and B. Image D

(J123, 1.5kx) captures the smooth and rod wax morphologies of the adaxial surfaces. Image E (J117, 1.5kx) is of a stoma and surrounding abaxial needle coated with the tubular wax morphology and was taken of the exposed stomata in image B. These tubular waxes are most consistent with an *n*-nonacosan-10-ol composition. Image F (J123, 5kx) captures these tubular waxes at a higher magnification that cover the adaxial and covered abaxial surfaces.

Figure 5. $\varepsilon^{13}C_{n\text{-C33 alkane}}$, $\delta^{13}C_{n\text{-C33 alkane}}$, and $\delta^{13}C_{leaf}$ values by growth treatment. Samples are represented using box and whisker plots with the median, upper and lower quartiles, and maximum and minimum values indicated. Median values are indicated next to box plots.

Figure 1

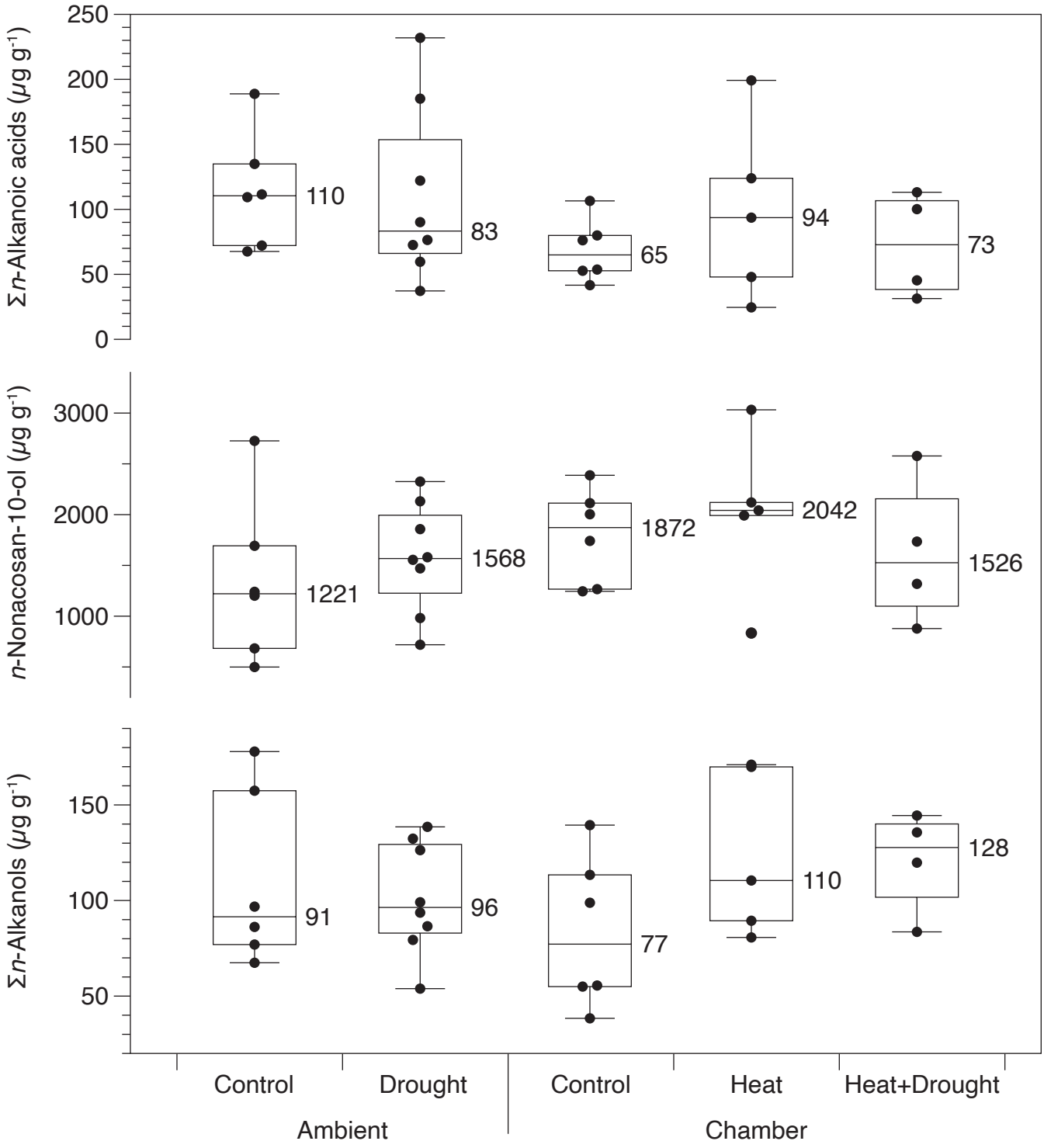

Figure 2

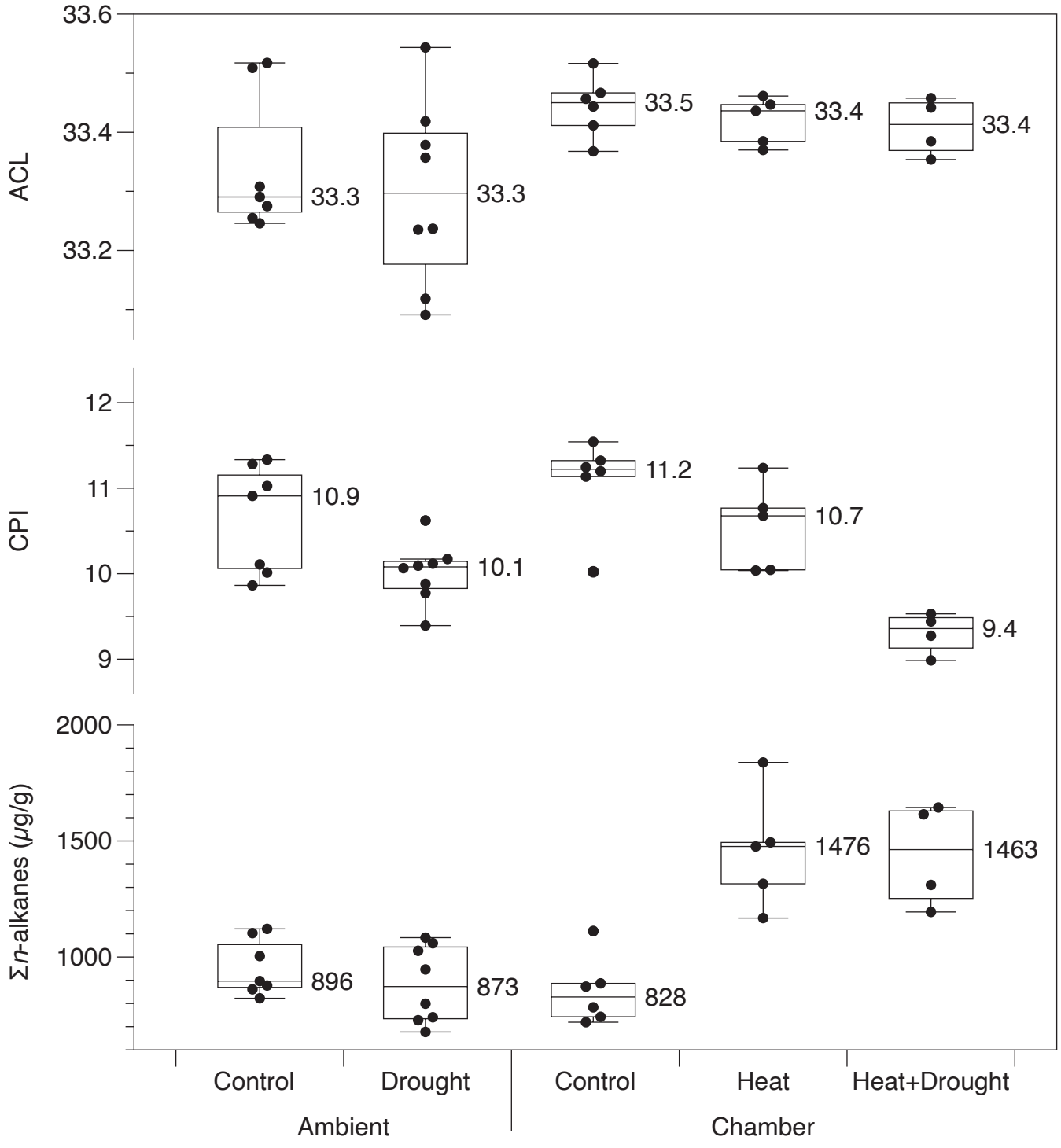

Figure 3

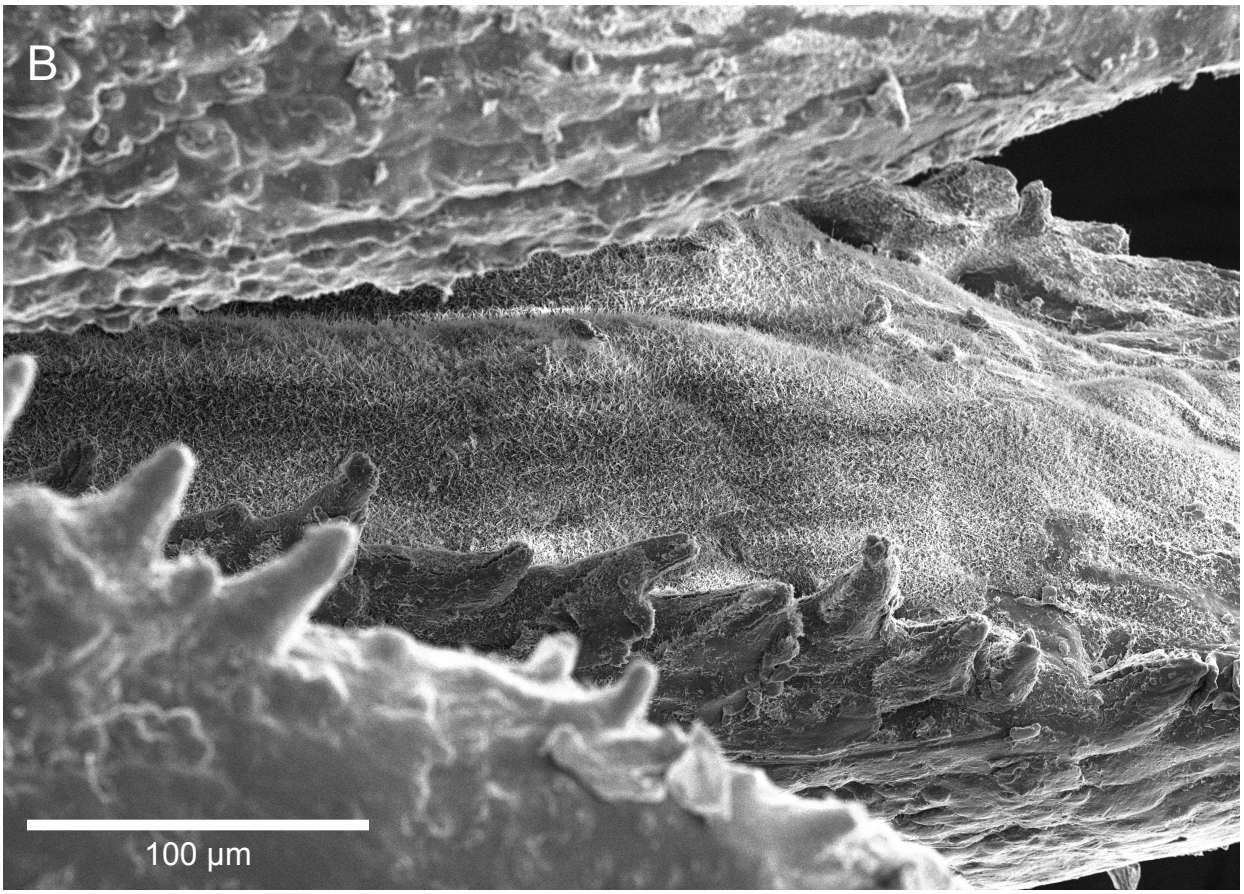

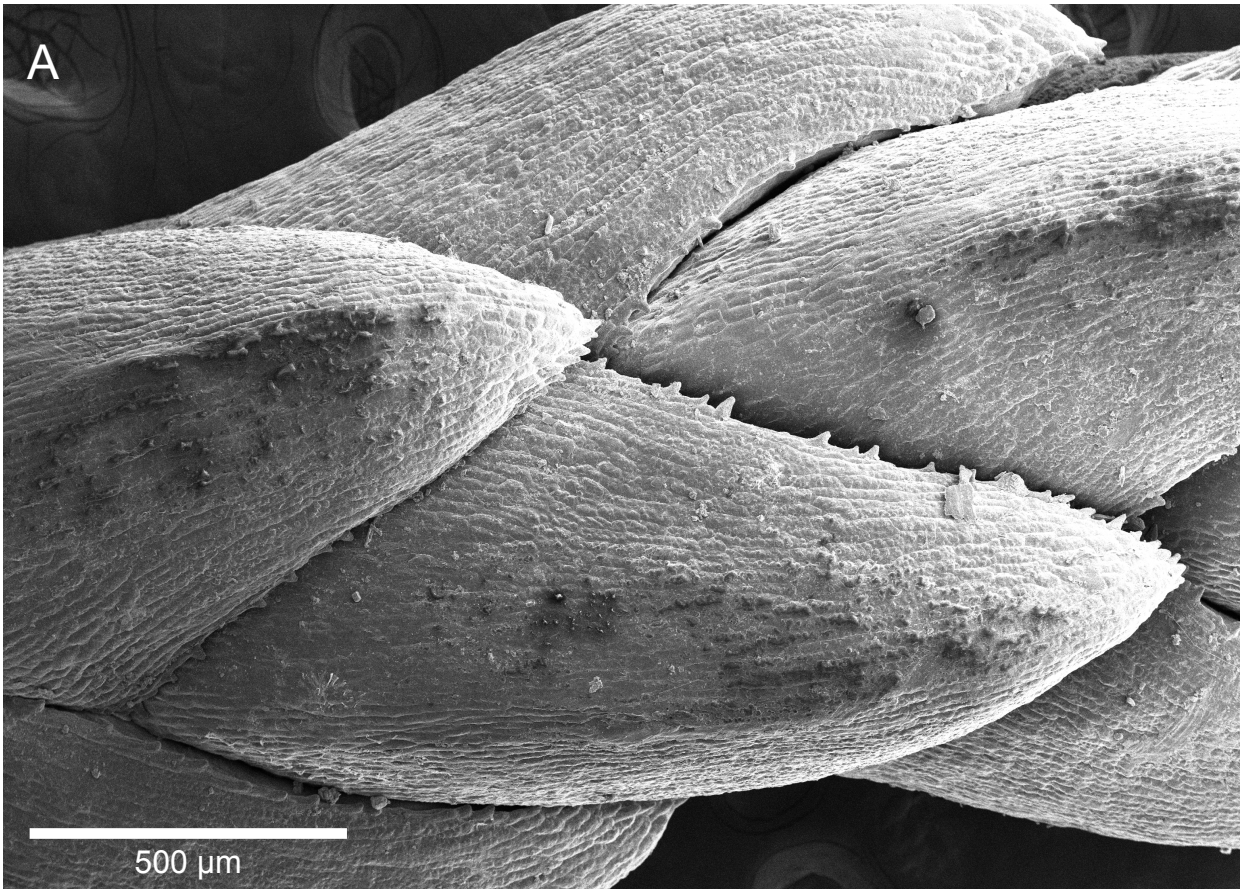

Figure 4

Click here to access/download;Figure;Figure 4 SEM 2020.pdf

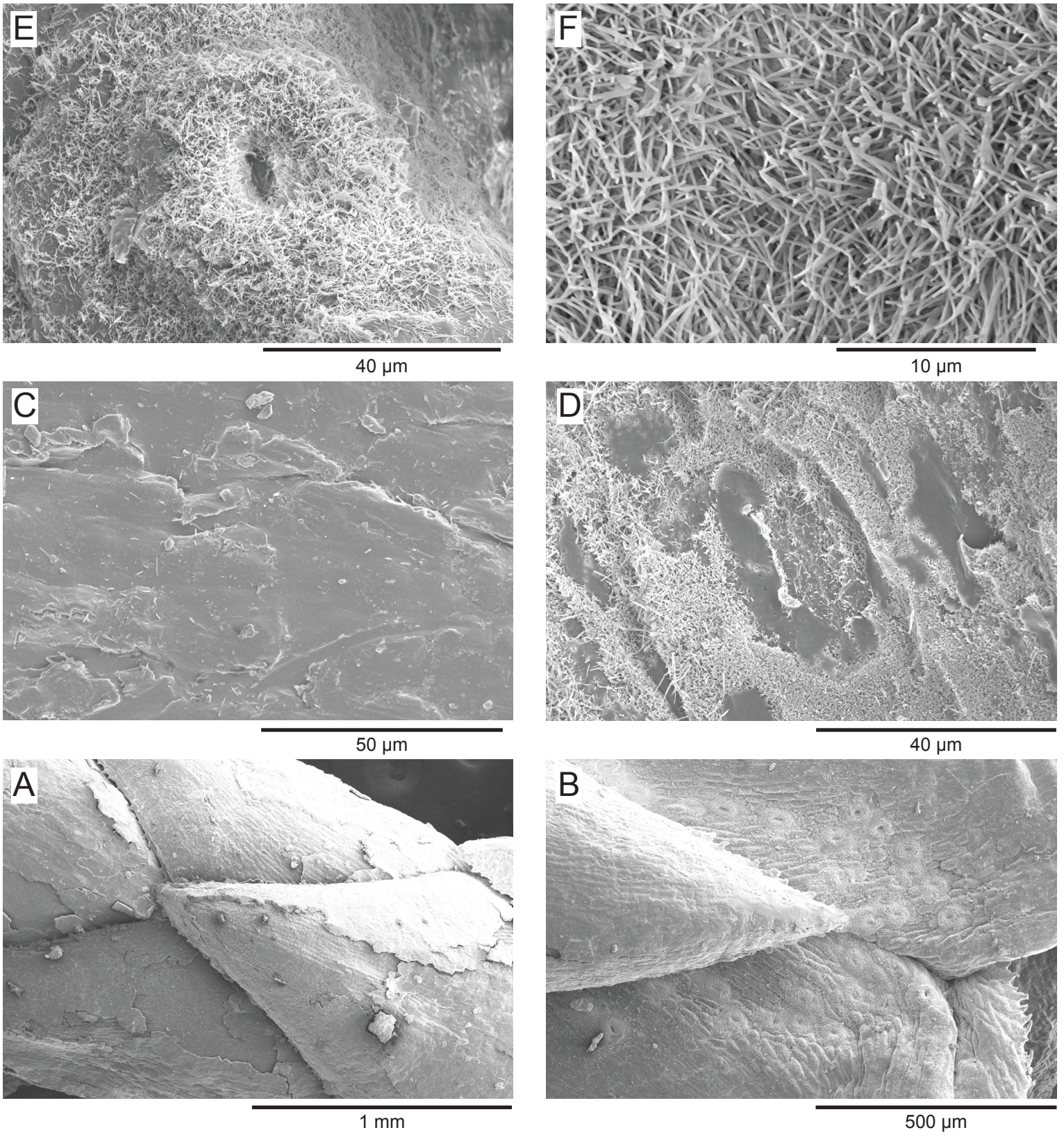

Figure 5

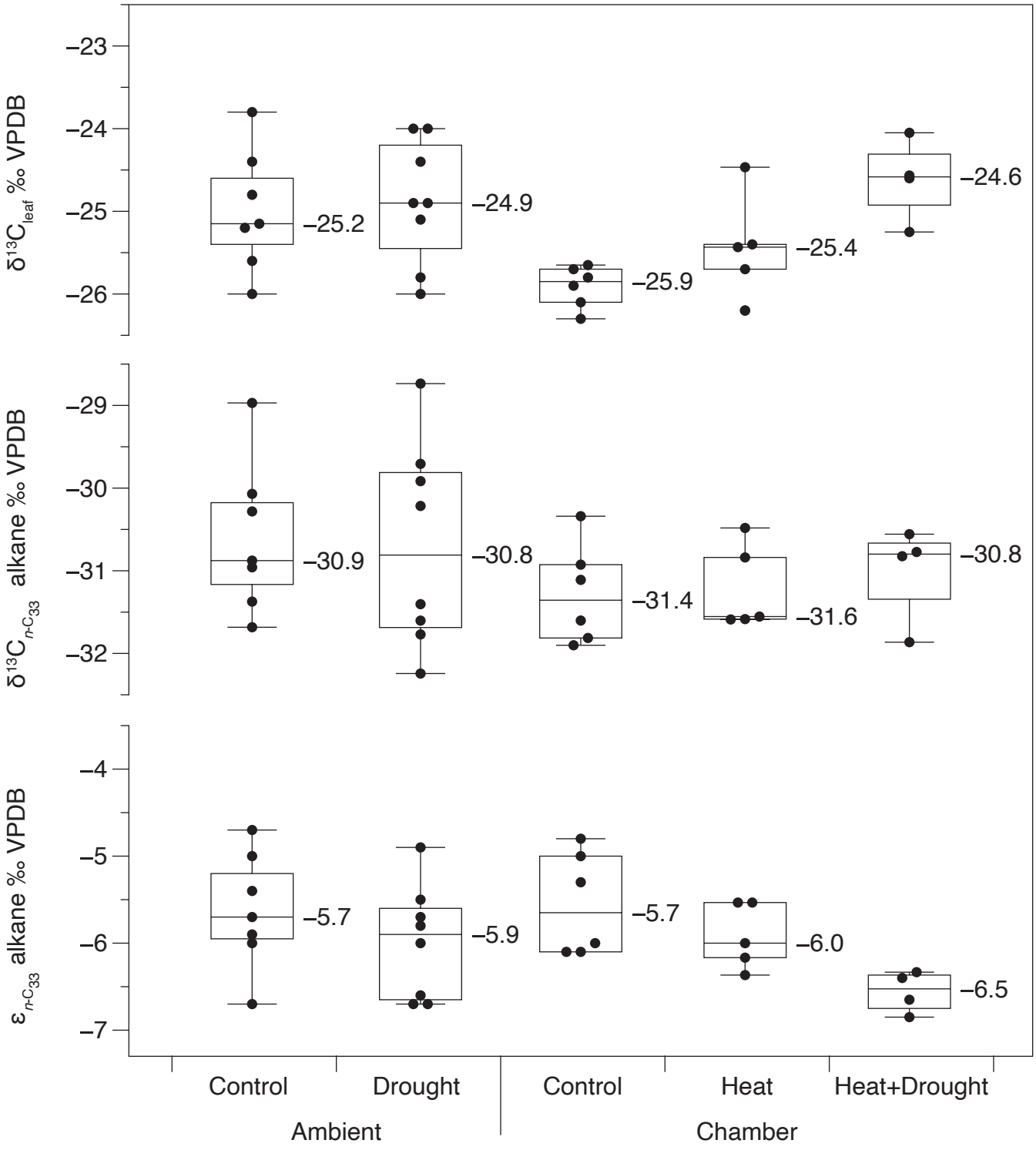

Table 1
Plant wax concentrations and *n*-alkane characteristics (ACL, CPI) for the different treatments.

Treatment	Σ*n*-Alkanes			ACL			CPI			Σ*n*-Alkanols			Nonacosan-10-ol			Σ*n*-Alkanoic acids		
	µg g^{-1}									µg g^{-1}			µg g^{-1}			µg g^{-1}		
	Mean	1σ	n[a]	Mean	1σ	n[a]	Mean	1σ	n[a]	Mean	1σ	n[a]	Mean	1σ	n[a]	Mean	1σ	n[a]
Ambient Control	955	121	7	33.3	0.1	7	10.6	0.6	7	110	46	6	1340	802	6	114	45	6
Drought	883	165	8	33.3	0.2	8	10.0	0.4	8	101	29	8	1578	541	8	109	67	8
Chamber Control	853	144	6	33.4	0.1	6	11.1	0.5	6	83	40	6	1793	465	6	68	24	6
Heat	1458	250	5	33.4	0.0	5	10.6	0.5	5	124	44	5	2004	781	5	98	69	5
Heat+Drought	1441	223	4	33.4	0.0	4	9.3	0.2	4	121	27	4	1627	724	4	73	40	4

[a] n is the number of individual trees per treatment. Many of the individual trees had multiple samples and these were averaged prior to statistical analysis. The total number of these replicates varied by individual and by compound analyzed (See Supplementary Table S1).

Table 2
Leaf and *n*-alkane $\delta^{13}C$ and $\varepsilon^{13}C$ values for the different treatments.

Treatment	‰ VPDB														
	$\delta^{13}C_{Leaf}$			$\delta^{13}C$ *n*-C33 Alkane			$\delta^{13}C$ *n*-C35 Alkane			$\varepsilon^{13}C$ *n*-C33 Alkane			$\varepsilon^{13}C$ *n*-C35 Alkane		
	Mean	1σ	n[a]	Mean	1σ	n[a]	Mean	1σ	n[a]	Mean	1σ	n[a]	Mean	1σ	n[a]
Ambient Control	–25.0	0.7	7	–30.6	0.9	7	–29.7	0.8	7	–5.6	0.7	7	–4.7	0.6	7
Drought	–24.9	0.7	8	–30.7	1.2	8	–29.9	1.2	8	–6.0	0.6	8	–5.1	0.7	8
Chamber Control	–25.9	0.2	6	–31.3	0.6	6	–30.9	0.6	6	–5.6	0.6	6	–5.1	0.5	6
Heat	–25.4	0.6	5	–31.2	0.5	5	–30.0	0.5	5	–5.9	0.4	5	–4.7	0.5	5
Heat+Drought	–24.6	0.5	4	–31.0	0.6	4	–29.9	0.7	4	–6.6	0.2	4	–5.4	0.3	4

[a] n is the number of individual trees per treatment. Many of the individual trees had multiple samples and these were averaged prior to statistical analysis. The total number of these replicates varied by individual and by compound analyzed (See Supplementary Table S1).